The *Ity/Lsh/Bcg* Locus: Natural Resistance to Infection with Intracellular Parasites Is Abrogated by Disruption of the *Nramp1* Gene

By Silvia Vidal,*‡ Michel L. Tremblay,* Gregory Govoni,*‡ Susan Gauthier,* Giovanna Sebastiani,*‡ Danielle Malo,‡ Emil Skamene,‡ Martin Olivier,‖ Serge Jothy,§ and Philippe Gros*‡

*From the *Department of Biochemistry, ‡Center for the Study of Host Resistance, §Department of Pathology, McGill University, Montreal, Québec, Canada H3G 1Y6; and ‖Service d'Infectiologie, Centre Hospitalier de l'Université de Laval, Ste-Foy, Québec, Canada G1K 7P4*

Summary

In mice, natural resistance or susceptibility to infection with intracellular parasites is determined by a locus or group of loci on chromosome 1, designated *Bcg*, *Lsh*, and *Ity*, which controls early microbial replication in reticuloendothelial organs. We have identified by positional cloning a candidate gene for *Bcg*, *Nramp1*, which codes for a novel macrophage-specific membrane transport protein. We have created a mouse mutant bearing a null allele at *Nramp1*, and we have analyzed the effect of such a mutation on natural resistance to infection. Targeted disruption of *Nramp1* has pleiotropic effects on natural resistance to infection with intracellular parasites, as it eliminated resistance to *Mycobacterium bovis*, *Leishmania donovani*, and lethal *Salmonella typhimurium* infection, establishing that *Nramp1*, *Bcg*, *Lsh*, and *Ity* are the same locus. Comparing the profiles of parasite replication in control and $Nramp1^{-/-}$ mice indicated that the $Nramp1^{Asp169}$ allele of Bcg^s inbred strains is a null allele, pointing to a critical role of this residue in the mechanism of action of the protein. Despite their inability to control parasite growth in the early nonimmune phase of the infection, $Nramp1^{-/-}$ mutants can overcome the infection in the late immune phase, suggesting that *Nramp1* plays a key role only in the early part of the macrophage–parasite interaction and may function by a cytocidal or cytostatic mechanism distinct from those expressed by activated macrophages.

A better understanding at the molecular level of the host mechanisms of defense against infection may open new therapeutic avenues for intervention in diseases in which drug resistance is a major impediment to treatment. The genetic analysis in mouse models of natural variations in innate susceptibility or resistance to various parasitic, bacterial, or viral infections provides a rational approach to the identification and characterization of such mechanisms (for review see reference 1).

One of the best studied genetic determinants of natural resistance or susceptibility to infectious diseases is the *Bcg* gene (2). *Bcg* is a single gene that is present in two allelic forms in the mouse (resistant, Bcg^r, and susceptible, Bcg^s) and determines innate resistance/susceptibility of mice to infection with several mycobacterial species such as *Mycobacterium bovis* (bacille Calmette-Guerin [BCG][1]), *M. lepraemurium*, and *M. intracellulare* (2–4). In inbred mouse strains, infection with *M. bovis* (BCG) is biphasic, with an early nonimmune phase (0–3 wk) characterized either by rapid proliferation of the bacteria in reticuloendothelial (RE) organs (liver, spleen) of Bcg^s, or by absence of bacterial growth in Bcg^r mouse strains (2). The late phase (3–6 wk), characterized either by complete clearance of the bacterial load or by persistent infection in the RE organs of the susceptible strains, is controlled by H-2–linked immune response genes (5, 6). Genetic linkage studies have shown that *Bcg* is either allelic or very tightly linked to two other host resistance loci, *Lsh* (7) and *Ity* (8). Similar to *Bcg*, *Lsh* controls the replication of *Leishmania donovani* in the RE organs, early in the nonimmune phase of infection (7). *Ity* also influences the early replication of *Salmonella typhimurium* in RE organs, but in this case animals either survive (resistant; Ity^r) or succumb rapidly (susceptible; Ity^s) to an infectious inoculum (8). In vitro (9–11) and in vivo (12–14) studies have shown that *Bcg*, *Ity*, and *Lsh* affect the capacity of the macrophage to restrict the intracellular replication of these antigenically unrelated intracellular parasites.

[1] *Abbreviations used in this paper:* BCG, bacille Calmette-Guerin; ES, embryonic stem; LDU, Leishman-Donovan units; mRNA, messenger RNA; P/L, phagosome/lysosome; TM, transmembrane.

S. Vidal and M. L. Tremblay contributed equally to this work.

We have used positional cloning to isolate candidate genes for *Bcg*. This approach was based on the construction of high resolution linkage (15) and physical maps (16) of the *Bcg* region on mouse chromosome 1, and on the isolation and characterization of cloned segments of the minimal physical interval in YAC clones (17). Briefly, exon trapping was used to identify seven candidate transcription units for *Bcg*. Of these genes, two were ubiquitously expressed in all tissues including RE organs, while one encoded a messenger RNA (mRNA) exclusively expressed in RE organs and, most importantly, in macrophages derived from them (17). This gene, designated *Nramp* (natural resistance-associated macrophage protein) encoded a novel integral membrane protein with 12 putative transmembrane (TM) domains, a glycosylated extracellular loop, and several phosphorylation sites (17). In addition, *Nramp* shares, through the presence of a consensus sequence signature, homology to a number of eukaryotic and prokaryotic membrane transport proteins, including a nitrate/nitrite concentrator of the fungus *Aspergillus nidulans* (18). Therefore, *Nramp* seems to be a novel macrophage-specific transport protein. Recently, we have determined that *Nramp* is part of a small gene family of at least two genes in the mouse, with a second gene *Nramp2* on chromosome 15 (19), and we have consequently renamed the chromosome 1 locus *Nramp1* (19).

Since the Bcg^s and Bcg^r genotypes and phenotypic characteristics are not unique to a specific mutant strain, but rather separate inbred strains in two nonoverlapping groups, we have analyzed a total of 27 Bcg^s and Bcg^r mouse strains for nucleotide sequence variations within the coding portion of *Nramp1* (20). One G to A substitution at nucleotide position 596 resulting in the nonconservative replacement of Gly^{169} to Asp^{169} within TM4 was found to be in absolute association with the *Bcg* phenotype in 20 Bcg^r strains (Gly^{169}) and 7 Bcg^s strains (Asp^{169}) tested (20). Haplotype mapping using sequence polymorphism identified within *Nramp1* and 11 additional polymorphic markers from the region revealed that the 7 Bcg^s strains tested shared a conserved core haplotype of 2.2 Mb overlapping *Nramp1* (20).

Although the replacement of a small neutral residue (glycine) by a bulkier, negatively charged one (aspartate) within one of the predicted TM domains of *Nramp1* would be likely to affect function, it does not per se constitute an obvious loss of function, and a full-length polypeptide is expected to be synthesized in Bcg^s mice. Therefore, we have used gene targeting to create a null allele at the *Nramp1* locus with the intent (*a*) to determine if *Nramp1* and *Bcg* are indeed allelic; (*b*) to determine if *Bcg*, *Lsh*, and *Ity* are allelic; and (*c*) to compare the phenotypic expression of $Nramp1^{Asp169}$ and *Nramp1* null mutations.

Materials and Methods

Design of Targeting Vector. The targeting vector pMC.NR was derived from the plasmid pMC1*neo*-polyA and the *Nramp1* genomic clone λnrp1. pMC1*neo*-polyA (Stratagene, La Jolla, CA) contains a 1-kb cassette with the structural neomycin resistance gene (*neo*) under the control of the Herpes simplex thymidine kinase (HSV-*tk*) gene promoter and followed at its 3′ end by a polyadenylation signal. The genomic DNA clone λnrp1 (Gros, P., and G. Govoni, unpublished data) was isolated from a 129sv/J mouse genomic library constructed in bacteriophage vector λDASH (Stratagene). It contains a 17-kb DNA insert overlapping exons 3–15 from the *Nramp1* gene. The longer genomic arm of pMC.NR was a 5-kb *Nramp1* fragment from intron 8 to within exon 15 cloned into the BamHI site of pMC1*neo*-poly(A). The shorter genomic arm of pMC.NR was a 1.1-kb SalI to HindIII *Nramp1* fragment extending from intron 4 to within exon 7. The cohesive ends of the 1.1-kb fragment were repaired with T4 DNA polymerase before ligation into the blunted XhoI site of the vector. The short *Nramp1* genomic arm provides a unique NotI site that originates from the polylinker of the λDASH vector. The two *Nramp1* genomic fragments were cloned so that their transcriptional orientation was the same as that of the *neo* cassette. Before transfection into embryonic stem (ES) cells, the construct was linearized by NotI digestion and dissolved in sterile water.

ES Cell Culture and Electroporation. The 129sv ES cell line J1 (21) was seeded onto a mitomycin C (Sigma Chemical Co., St. Louis, MO)–inactivated embryonic fibroblast feeder cell layer (2 h at 37°C) in DMEM (GIBCO BRL, Gaithersburg, MD) containing 500 U/ml leukemia inhibitory factor (GIBCO BRL) and 15% heat-inactivated FCS (GIBCO BRL). For electroporation, ES cells were trypsinized and resuspended (10^7 cells/ml) in PBS. 1 ml of the cell suspension was mixed with pMC.NR-linearized DNA at a concentration of 50 μg/ml and electroporated using a Gene Pulser (Bio-Rad Laboratories, Richmond, CA) with a setting of 500 μF capacitance, 240 mV (22). ES cells were then plated at a density of 2×10^5 cells per 60-mm dish onto a monolayer of neomycin-resistant, mitotically inactive fibroblast feeder cells. Selection for *neo*+ clones was initiated 24 h later by addition of geneticin (G418; GIBCO BRL; final concentration 500 μg/ml). 5–10 $G418^R$ colonies per plate were picked 10 d after electroporation and sequentially expanded in 96- and 24-well titer plates. Each clone was recovered by trypsin treatment and then frozen at −80°C in culture medium supplemented with 10% DMSO and 20% FCS.

Genotyping of ES Cell Lines and Mutant Mice. Genomic DNA from individual ES clones was directly isolated onto replica 96-well plates according to the procedure of Ramirez-Solis et al. (23), dissolved in 30 μl of restriction enzyme buffer (recommended by the supplier of enzyme) containing 1 mM spermidine and 100 μg/ml BSA, and digested with 20 U of either BamHI or XbaI (incubation 16 h, 37°C). Genomic DNA was isolated from mouse tails by a standard protocol (24) using proteinase K digestion, phenol extraction, and ethanol precipitation. Restricted DNA from ES cell clones or mouse tails was resolved by electrophoresis in 1% agarose gels containing TAE buffer (40 mM Tris-acetate, 20 mM sodium acetate, 20 mM EDTA, pH 7.6), and transferred onto nylon membranes (Hybond-N; Amersham International, Little Chalfont, UK) by capillary blotting in 20× SSC (1× SSC is 0.15 M NaCl, 0.015 M sodium citrate). Southern blots were prehybridized for 16 h at 42°C and then hybridized for 16 h at 42°C in the same mixture composed of 50% formamide, 5× SSC, 1% SDS, 10% dextran sulfate, 20 mM Tris-HCl, pH 7.5, 1× Denhardt's solution (0.1% BSA, 0.1% Ficoll, 0.1% polyvinylpyrrolidone), and heat-denatured salmon sperm DNA at a final concentration of 200 μg/ml. The *Nramp1* hybridization probe was a cDNA fragment (nucleotide 300 to 550; 17) labeled to high specific activity (1×10^9 cpm/μg DNA) by random priming (25) with α-[^{32}P]dATP (specific activity 3,000 Ci/mmole), and used at 1×10^6 cpm/ml of hybridization solution. The membranes were washed to a final stringency of 0.5× SSC, 0.1% SDS at 65°C for 30 min.

Blastocyst Injection and Animal Breeding. Blastocysts were obtained

3.5 d after coitus from pregnant 6-wk-old BALB/c females obtained by natural mating with syngeneic males. 10–15 ES cells from two independent clones, EP1-26 and EP2-173, were microinjected into each blastocoel cavity (26). The blastocysts were then reimplanted into the uterine horn of pseudopregnant CD1 mice. Chimeric offspring were identified by the agouti contribution of the ES cells to the coat color, and chimeric males were crossed with BALB/c females to produce a (129sv × BALB/c) F1 generation bearing one *Nramp1* null allele (*Nramp1*$^{-/Asp169}$). Germline transmission was determined by the presence of agouti mice in the offspring. The genotype of this offspring was determined by tail blot, and *Nramp1*$^{-/Asp169}$ carrier animals were either backcrossed to BALB/c animals to expand the heterozygous *Nramp1*$^{-/Asp169}$ population or intercrossed to generate homozygous F2 null mutant mice (*Nramp1*$^{-/-}$). Mutant F1 (*Nramp1*$^{-/Asp169}$) and F2 (*Nramp1*$^{-/-}$) animals were genotyped and then tested for susceptibility to infection with intracellular parasites.

RNA Hybridization Studies. Total cellular RNA was isolated from frozen spleens after homogenization with a mortar and pestle precooled with liquid nitrogen. The tissue powder was dissolved in guanidinium hydrochloride (6 M), and RNA was recovered by differential ethanol precipitation and phenol and chloroform extractions (27). RNA was separated by electrophoresis in a denaturing formaldehyde agarose gel and transferred to a nylon membrane (GeneScreen Plus, E. I. du Pont de Nemours & Co., Inc., Wilmington, DE), and the blot was prehybridized (16 h, 65°C) and hybridized (16 h, 65°C) in the same solution consisting of 1 M NaCl, 1% SDS, and 10% dextran sulfate. The hybridization probe was a mouse *Nramp1* cDNA subfragment overlapping exons 7 and 8 (nucleotide 855–1064; 17), was labeled to high specific activity with α-[^{32}P]dATP, and was used at 2 × 10^6 cpm/ml hybridization solution. The blot was washed under conditions of increasing stringency up to 0.5× SSC, 0.1% SDS at 65°C for 45 min.

Infection of Mice with BCG, L. donovani, and S. typhimurium. The BCG infectious inoculum consisted of a single-cell suspension of *M. bovis* (BCG, strain Montreal) prepared by microfiltration from two serial 7-d cultures in Dubos oleic acid medium, as previously described (2). Mice were inoculated in the caudal tail vein with 0.25 ml of a BCG suspension containing 1.4 × 10^4 CFU/ml in physiological saline. The degree of infection was assessed by determining the number of spleen colony-forming units at predetermined time intervals (2). Geometric means plus or minus standard deviation of spleen BCG CFUs were calculated from five infected animals per time point.

The virulent strain *L. donovani infantum* Ethiopian LV9 was passaged continuously by intraperitoneal infection of Syrian hamsters and was generously donated by Dr. G. Matlashewski (Institute of Parasitology, McGill University, Montreal, Canada). The infectious inoculum was prepared from spleen homogenates of infected hamsters according to the procedure of Murray et al. (28) and used immediately to infect mice intravenously (caudal tail vein, 0.2 ml volume of a suspension of 5 × 10^7/ml infectious *L. donovani* amastigotes). At different times (1, 3, and 6 wk) after infection, livers were removed, weighed, and sectioned for impression smears. The extent of disease was quantitated by microscopic determination of the number of parasites in Giemsa-stained liver impression smears. Hepatic parasite burden was expressed in Leishman-Donovan units (LDU, the number of parasites per 1,000 nucleated cells × liver weight in milligrams; 28). A minimum of four mice were used for each infection time point and for each experimental group.

The highly virulent *S. typhimurium* strain Keller (29) was originally obtained from Dr. Hugh Robson (Royal Victoria Hospital, Montreal, Canada). Mice were injected intravenously (caudal tail vein) with a 0.2-ml inoculum containing 5 × 10^4 CFU/ml *S. typhimurium*. Animals were examined twice a day for a period of up to 4 wk, and deaths were recorded and moribund animals were killed. Resistance to infection was assessed by the percentage of surviving animals among groups of 5–15 mice. *Ity*^{s} animals typically succumbed to infection within 4–6 d, while *Ity*^{r} animals typically survived at least 14 d after infection.

Histopathology. Mice from various groups were killed by cervical dislocation and autopsied. The major organs, including spleen, liver, lung, intestine, colon, and thymus, were removed, immediately fixed in 10% formalin, and embedded in paraffin. Sections (5 μm) from paraffin blocks containing these organs were stained with hematoxylin and eosin for routine histological examination. Randomly selected (n = 10) high power fields (×100 and ×160) of tissue sections were examined from each animal. In addition, 5-μm sections of the spleen and liver were stained for the presence of mycobacteria by the Ziehl-Neelsen acid-fast stain.

Results

Disruption of the Nramp1^{Gly169} *Allele Associated with Resistance to Infection with Intracellular Parasites.* We used homologous recombination in ES cells to generate a mutant mouse carrying a null allele at the *Nramp1* locus (*Nramp1*$^-$) on the *Bcg*^{r} genetic background of the ES cell line J1 (21) from mouse strain 129sv (*Bcg*^{r}, *Nramp1*^{Gly169}, or *Nramp1*$^+$). Since the resistance *Bcg*^{r} allele is dominant over the susceptibility *Bcg*^{s} allele, the loss of resistance to infection after targeting of the *Nramp1*^{Gly169} allele associated with resistance (20) should unambiguously confirm that *Nramp1* and *Bcg* are the same gene. Our targeting strategy was based on that of Thomas and Capecchi (30) and used *neo* as a positive selectable marker. To construct the targeting vector pMC.NR, two noncontiguous *Nramp1* genomic fragments of size 1.1 kb (exons 5–7) and 5.0 kb (exons 9–15) were cloned into the plasmid pMC1*neo*-polyA on either side of the *neo* cassette (Fig. 1). Successful targeting of the *Nramp1* locus by homologous recombination using this construct should result in (*a*) deletion of a 500-bp *Nramp1* genomic DNA segment disrupting exon 7 and deleting exon 8; (*b*) insertion of the *neo* marker at that site and introduction of translation termination codons in three reading frames, resulting in a severely truncated protein lacking 8 of the 12 predicted TM domains; and (*c*) generation of novel RFLPs diagnostic for the targeted event.

Successful targeting of *Nramp1* was identified by Southern blotting of genomic DNA through the appearance of diagnostic 6.0-kb BamHI or 8.5-kb XbaI fragments hybridizing to an *Nramp1* cDNA probe (nucleotide 300–550; 17) external to the targeting construct. An example of this analysis is shown in Fig. 1 *B* in which the hybridization profiles of targeted and nontargeted (2–62) ES clones are compared. Two independent ES clones, 1-26 and 2-173, were used to produce chimeric mice by injection into expanded BALB/c blastocysts. Male chimeras were mated to BALB/c (*Nramp1*^{Asp169}) females, and the F1 progeny scored for successful germline transmission of the targeted *Nramp1* allele (agouti color). Since the *Bcg*^{r} allele is dominant, the appearance of animals susceptible to infection in heterozygous carriers (*Nramp1*$^{-/Asp169}$)

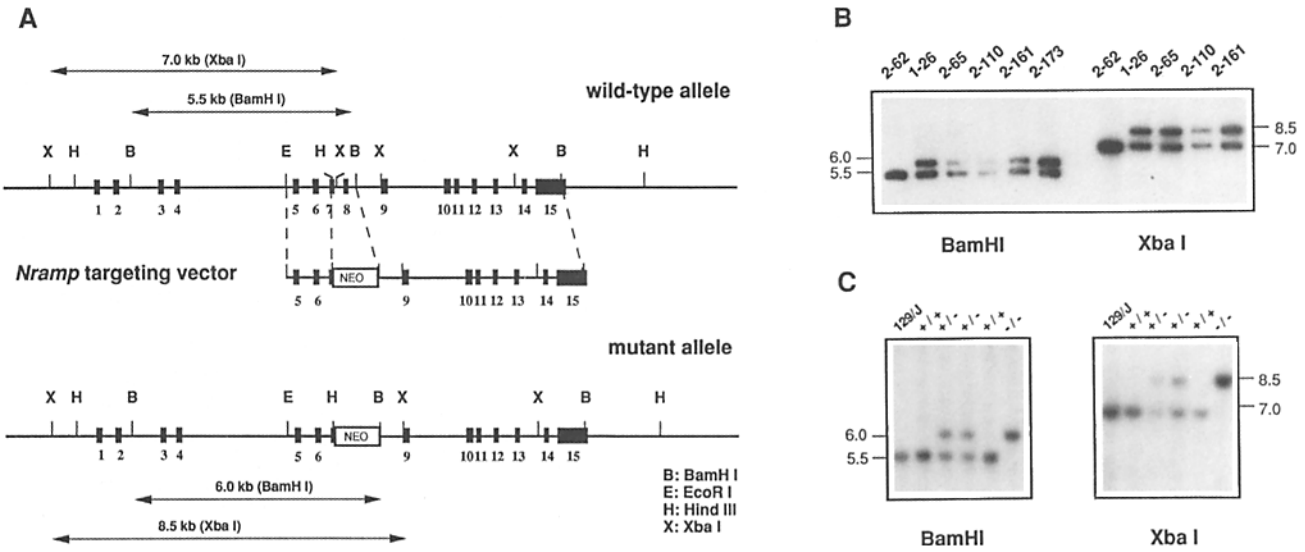

Figure 1. Creation of a null allele at the *Nramp1* locus by homologous recombination. (*A*) Targeting strategy. The genomic structure of the mouse *Nramp1* locus is shown with the genomic exons numbered 1–15 and identified as dark boxes (wild-type allele). A diagram of the *Nramp1*-targeting vector showing the *neo* expression cassette flanked by a proximal 1.1-kb fragment that includes exons 5 and 6 and part of exon 7 on one side, and a 5.0-kb fragment that includes exons 9–15 on the other side, is shown below the wild-type allele map. The genomic organization of the corresponding mutant allele generated by successful homologous recombination at *Nramp1* in ES cells is presented. Restriction enzymes sites for BamHI (*B*), EcoRI (*E*), HindIII (*H*), and XbaI (*X*) are identified in both alleles. The position of key genomic XbaI and BamHI restriction DNA fragments diagnostic of the wild-type (7.0-kb XbaI, 5.5-kb BamHI) and the mutant *Nramp1* allele (8.5-kb XbaI, 6.0-kb BamHI) targeted by homologous recombination and recognized by a cDNA hybridization probe overlapping exons 3–4 (positions 300–550; 17) are indicated immediately above and below the corresponding genomic maps of the two alleles. (*B*) *Nramp1* targeting in ES cells. Results of Southern blotting analysis of genomic DNA from independent G418-resistant ES cell clones digested with either BamHI or XbaI and hybridized to a *Nramp1* cDNA fragment (positions 300–550; 17) are shown. Successful targeting is evidenced for clones 1-25, 2-65, 2-110, 2-161, and 2-172 by the presence of diagnostic 6-kb BamHI- and 8.5-kb XbaI-hybridizing fragments on the background of the endogenous 5.5-kb BamHI and 7.0-kb XbaI fragments. (*C*) Creation *Nramp1* mutant mice. Results of Southern blotting analysis of genomic DNA from control 129sv mouse strain and individuals from a (129sv × BALB/c) F2 cross in which the wild-type allele of 129sv had been successfully targeted by homologous recombination are shown. Offspring from this cross include heterozygotes (−/+) and homozygotes (−/−) for the targeted allele *Nramp1*$^{-}$. The *Nramp1* cDNA probe and diagnostic hybridizing restriction fragments are as described in *B*.

would demonstrate allelism between *Nramp1* and *Bcg*. Homozygous null mutants (*Nramp1*$^{-/-}$) were obtained by intercrossing independently heterozygotes derived from either 1-26 or 2-173 ES cell clones, and the null *Nramp1*$^{-/-}$ genotype was verified by Southern blotting (Fig. 1 *C*). Homozygous *Nramp1*$^{-/-}$ null mice were housed in a barrier facility and were free of specific mouse pathogens. Under these conditions, the general health and viability of *Nramp1*$^{-/-}$ mice appeared normal up to 14 mo of age.

Wild-type Nramp1 mRNA Transcripts Are Absent from Nramp1$^{-/-}$ *Null Mice.* To verify that intact *Nramp1* mRNA was indeed absent from mutant mice, Northern blotting analysis of total spleen RNA from wild-type, heterozygous, and homozygous mutant mice was carried out using a hybridization probe corresponding to exons 7 and 8 of the gene, which are deleted by the targeting event (nucleotide 855–1064; 17) (Fig. 2 *A*). The spleen was chosen as a source of RNA since it is the strongest site of endogenous *Nramp1* mRNA expression in normal mouse tissues (17). Results from this analysis (Fig. 2 *A*) indicated that the 2.4-kb *Nramp1* mRNA was abundant in spleen from wild-type animals and that its level was reduced by ~50% in heterozygotes (*Nramp1*$^{-/+}$), whereas it could not be detected in homozygous null (*Nramp1*$^{-/-}$) mice, even upon prolonged exposure of the blot (data not shown). The reduction in or absence of *Nramp1* mRNA detected by Northern blotting with this probe was not due to absence of RNA in the lanes, since reprobing of the blot with a control GAPDH cDNA probe revealed equal RNA loading and transfer to the membrane in each lane (Fig. 2 *C*). These results indicate that no wild-type *Nramp1* mRNA transcripts are produced in homozygous null mutants. Rehybridization of the blot with a *neo* gene probe or a probe corresponding to exon 5 of *Nramp1* revealed the presence of several novel mRNAs that were specific to the targeted gene and were absent from spleens of control BALB/c mice (Fig. 2 *B* and data not shown). These transcripts most likely either represent hybrid *neo-Nramp1* mRNAs or result from alternative splicing of the *neo* cassette in the targeted gene. However, either event would result in the production of RNAs recruiting different reading frames, resulting in the appearance of termination codon within exon 9, producing a mature Nramp1 protein that is severely truncated (lacking the carboxy-terminal half) and probably nonfunctional.

Organ Morphology of Nramp1$^{-/-}$ *Null Mice.* Mouse *Nramp1* is expressed primarily in macrophages, professional phagocytic cells which populate all tissues of the host. These

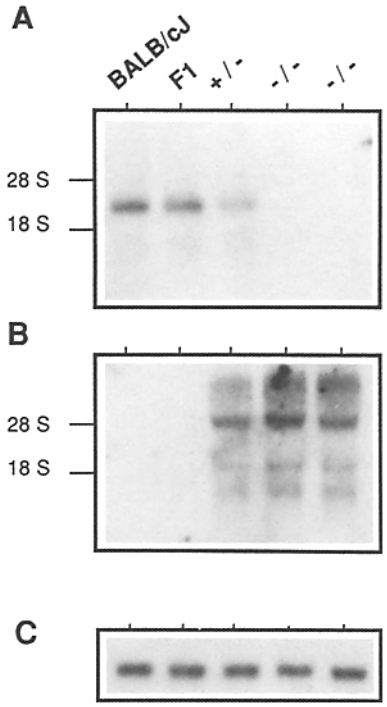

Figure 2. Absence of wild-type *Nramp1* mRNA transcripts in targeted mice. 20 μg of total cellular RNA from spleen of control BALB/cJ, control (129sv × BALB/cJ) F1 mice, and animals from a (129sv × BALB/c) F2 cross, either heterozygous (*Nramp1*$^{-/Asp169}$) or homozygous (*Nramp1*$^{-/-}$) for a null allele at *Nramp1*, was separated by agarose gel electrophoresis and analyzed by Northern blotting. (*A*) The hybridization probe corresponds to a portion of *Nramp1* exons 7 and 8 that is deleted by homologous recombination at the *Nramp1* locus, using the targeting vector described in Fig. 1 *A*. The 2.4-kb *Nramp1* mRNA transcript is identified in control groups and in the heterozygous null mutant. The same blot was rehybridized to control cDNA probes corresponding either to the *neo* gene probe present in the targeting vector (*B*) or to the cellular glyceraldehyde phosphate dehydrogenase gene (*C*).

cells not only play a key role as a first line of defense against intracellular parasites but also participate in other key physiological events such as adaptive immune response and normal development of certain organs and structures. Although homozygous *Nramp1*$^{-/-}$ null mice were viable and fertile, we analyzed possible deleterious effects of the absence of *Nramp1* on organ morphogenesis. Special attention was paid to the macrophage-rich RE organs, spleen and liver. The white and red pulp (Fig. 3, panel *1*) regions were well defined in the spleen of control and *Nramp1*$^{-/-}$ mutants, and distribution of specific cell populations within these regions was also preserved. Darkly stained cells are lymphocytes within the dense lymphoid tissues of the white pulp organized around small arterioles (Fig. 3, panel *2*), whereas weakly stained cells are macrophages, dendritic cells, sparse lymphocytes, and plasma cells scattered among vascular sinusoids, which together constitute the red pulp. Likewise, the normal architecture of the liver was maintained in *Nramp1*$^{-/-}$ animals (Fig. 3, panel *3*). Liver lobules show regular trabecular arrangement of hepatocytes of uniform size with hepatic macrophages, or Kupffer cells, lining the sinusoidal space (data not shown). Fig. 3, panels *4–7*, presents an analysis in *Nramp1*$^{-/-}$ mutants of other tissues that are not classified as RE organs but nevertheless contain biochemically and immunologically unique populations of macrophages. These include lung parenchyma (Fig. 3, panel *4*), thymus (Fig. 3, panel *6*), small intestine (Fig. 3, panel *5*), and colon (Fig. 3, panel 7). The integrity of these structures and cell populations was also found to be intact in *Nramp1*$^{-/-}$ mutant mice.

Disruption of the Nramp1^{Gly169} *Allele Abrogates Resistance to BCG Infection.* In mice, BCG infection in RE organs is biphasic, with an early phase (up to 3 wk) that is under *Bcg* gene control and is characterized by either rapid bacterial replication in *Bcg*^{s} mice or no bacterial proliferation in *Bcg*^{r} animals. The late or immune phase of infection is characterized by bacterial clearance from the spleen of *Bcg*^{s} mice, through the emergence of specific T cell–mediated immunity and bacillary destruction by activated macrophages. To assess the role of *Nramp1* in resistance to mycobacterial infections, the kinetics of BCG infection was followed in the spleen of either resistant control (129sv × BALB/c) F1 mice (*Nramp1*$^{+/Asp169}$), susceptible control BALB/c (*Nramp1*^{Asp169}) mice, or mice heterozygous for a null allele at *Nramp1* (*Nramp1*$^{-/Asp169}$). In control BALB/c mice, bacterial proliferation was rapid and uncontrolled in the early phase and reached a maximum at 3 wk (1.5×10^5 BCG CFU/spleen), and the BCG load was decreased by 6 wk after infection (Fig. 4 *B*). On the other hand, in control resistant (129sv × BALB/c) F1 animals, little or no bacterial proliferation was observed in the spleen at any time during infection (maximal load, 3×10^3 CFU BCG/spleen) (Fig. 4 *A*). The profile of BCG infection in (129sv × BALB/c) F1 mice heterozygous for the null allele (*Nramp1*$^{-/Asp169}$) (Fig. 4 *C*) was indistinguishable from that of BALB/c control (Fig. 4 *B*), including rapid early BCG proliferation peaking at 3 wk (1.5×10^5 CFU BCG/spleen), followed by progressive elimination of the bacterial load. These results show that mice carrying a mutated *Nramp1*^{Gly169} allele (*Nramp1*$^{-/Asp169}$) lose their capacity to control BCG growth when compared with their littermates carrying the unmutated allele (*Nramp1*$^{+/Asp169}$), and they establish that *Nramp1* and *Bcg* are allelic.

BALB/c mice (*Bcgs*, *Nramp1*^{Asp169}) can mount efficient immune response and ultimately eradicate the spleen bacterial load (Fig. 4 *B*) in the late phase of infection, through a T cell–dependent macrophage activation process (31, 32). Should *Nramp1* also play a role in macrophage–mediated BCG killing in the late phase of infection, these observations suggest that the *Nramp1*^{Asp169} allele may only constitute a partial loss of function. Results shown in Fig. 4 indicate that the kinetics of BCG infection in homozygous *Nramp1*$^{-/-}$ mice (Fig. 4 *D*) was identical to that of BALB/c controls (Fig. 4 *B*) and of *Nramp1*$^{-/Asp169}$ heterozygotes (Fig. 4 *C*), strongly suggesting that the *Nramp1*^{Asp169} allele of *Bcg*^{s} mice is as severe a mutation as the *Nramp1*$^{-}$ allele.

Interestingly, data in Fig. 4 *D* also indicate that homozygous null mutants are able to stop BCG proliferation and initiate bacterial clearance in the late phase of infection. During this part of the BCG infection, infected macrophages syn-

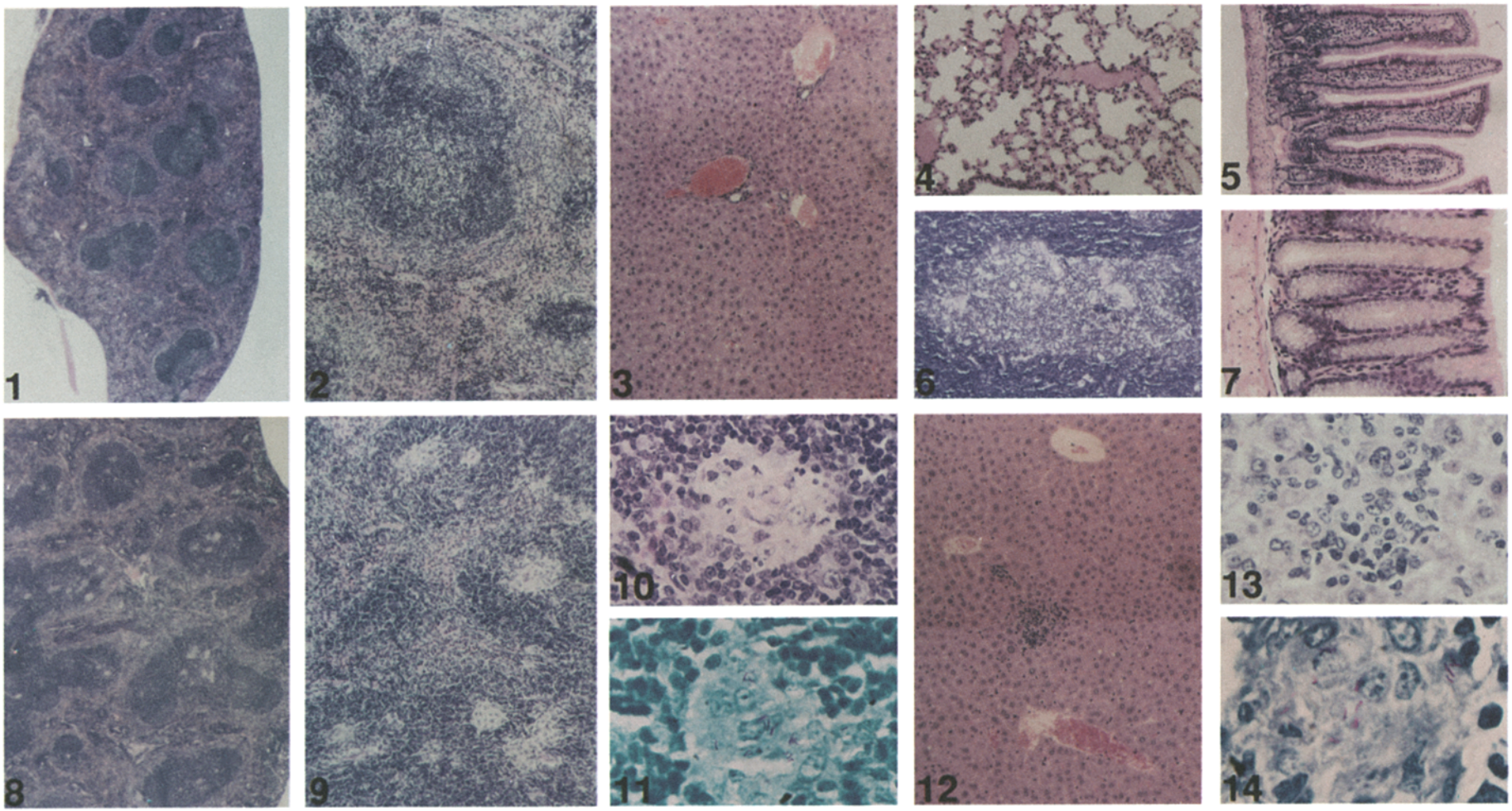

Figure 3. Histopathology of normal and BCG-infected *Nramp1* null mutant mice. Histologic sections (5 μm thick) of formalin-fixed, paraffin-embedded tissues were stained with hematoxylin-eosin for routine analysis (sections 1-10, 12-13) or with Zeihl-Neelsen for the presence of acid-fast bacilli (sections 11 and 14). The upper panel shows sections from uninfected animals corresponding to spleen (10×, panel *1*; 40×, panel *2*), liver (40×, panel *3*), lung parenchyma (panel *4*), thymus (panel *6*), small and large intestine (panels *5* and *7*, respectively; all 40×). The lower panel shows tissue section from RE organs of BCG-infected mice 3 wk after infection corresponding to spleen (10×, panel *8*; 40×, panel *9*), and liver (40×, panel *12*). Individual granulomas in spleen (panel *10*) and liver (panel *13*) are shown at higher magnification (160×), and mycobacteria included inside these granulomas (spleen, 200×, panel *11*; liver, 400×, panel *14*) are identified as red acid-fast bacilli by Zeihl-Neelsen staining.

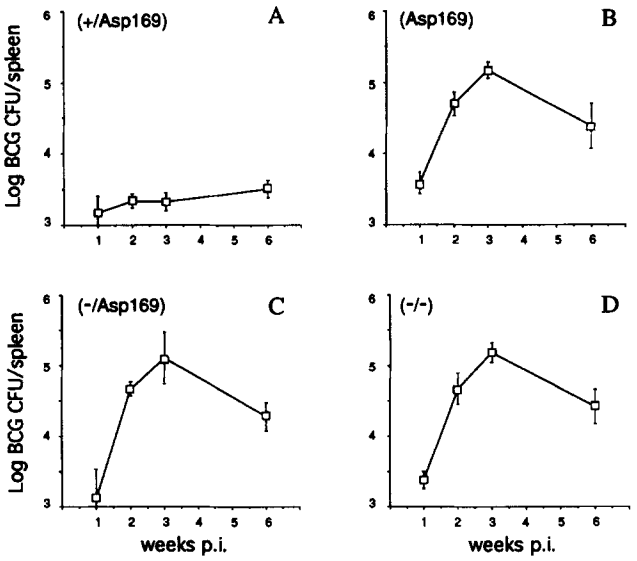

Figure 4. BCG infection in spleens of control mice and mice bearing targeted mutations at *Nramp1*. Groups of either control resistant (129sv × BALB/cJ) F1 (+/Asp169, *A*) or susceptible BALB/cJ mice (Asp169, *B*), and mice from a (129sv × BALB/cJ) F2 cross either heterozygous (−/Asp169, *C*) or homozygous (−/−, *D*) for a null allele at *Nramp1* were tested for resistance to infection with *M. bovis* (BCG). 2 × 10^4 live BCG bacilli were injected intravenously, and the number of live colony-forming units of BCG recovered from infected spleen was determined at different times after infection (*p.i.*). Results from individual groups of five mice were pooled, and the logarithm of the average number of colony-forming units (± standard errors) was calculated and is shown.

thesize cytokines, leading to T cell activation and further recruitment of monocytes to form granulomas, the primary site of infection, and, eventually, bacterial eradication in RE organs (immune phase). To analyze more closely this aspect of BCG infection in *Nramp1*$^{-/-}$ mice, a histological analysis of infected RE organs was carried out. All aspects of granuloma formation were found to be identical in *Nramp1*$^{-/-}$ and control BALB/c mice, with respect to site, number, morphology, and cell populations involved (Fig. 3). Granuloma formation was restricted to the spleen and liver of both groups of mice; a few small granulomas were detected as early as 2 wk (data not shown), while at 3 wk their number and size were maximal. Well-formed granulomas are shown for the spleen (Fig. 3, panels *9* and *10*) and liver (Fig. 3, panels *12* and *13*) and consist of large epitheloid cells (differentiated macrophages) and monocytes, arranged in a whirling and palisading pattern. Staining of these structures for acid-fast bacilli (Ziehl-Neelsen) revealed the presence of BCG bacilli within these granulomas in spleen and liver (Fig. 3, panels *11* and *14*, respectively). In both *Nramp1*$^{-/-}$ and control BALB/c mice, the number and size of granulomas had declined considerably by 6 wk after infection (data not shown). These results indicate that an intact *Nramp1* gene is not necessary to (*a*) mount cellular responses against BCG leading to granuloma formation; (*b*) contain bacterial dissemination; or (*c*) trigger macrophage differentiation into cells capable of killing ingested mycobacteria.

Disruption of the Nramp1^{Gly169} *Allele Has Pleiotropic Effects on Resistance to Intracellular Infections.* Genetic linkage studies have indicated that *Bcg* is tightly linked to two other host resistance loci, *Lsh* and *Ity* (33), which control natural resistance of mice to infection with *L. donovani* and *S. typhimurium*, respectively (7, 8). To determine if *Bcg/Ity/Lsh* are the same gene, we tested the effect of a null mutation at *Nramp1* on resistance to *L. donovani* and *S. typhimurium*.

To assess the role of *Nramp1* in resistance to *L. donovani*, the kinetics of *L. donovani* infection was followed in the liver of either resistant control (129sv × BALB/c) F1 (*Nramp1*$^{+/Asp169}$) mice, susceptible control BALB/c (*Nramp1*^{Asp169}) mice, or mice heterozygous for a null mutation at *Nramp1* (*Nramp1*$^{-/Asp169}$) (Fig. 5). In control BALB/c mice, *L. donovani* replication was rapid during the early phase and reached a maximum at 3 wk (average 1,400 LDU), and parasite counts had decreased by ~50% by 6 wk after injection (average 750 LDU) (Fig. 5 *A*). By contrast, little or no parasite proliferation was observed in the liver of control resistant (129sv × BALB/c) F1 animals throughout the 6-wk observation period (average 80 LDU at 1 wk versus 120 LDU at 6 wk) (Fig. 5 *B*). Results shown in Fig. 5 *C* show that in the heterozy-

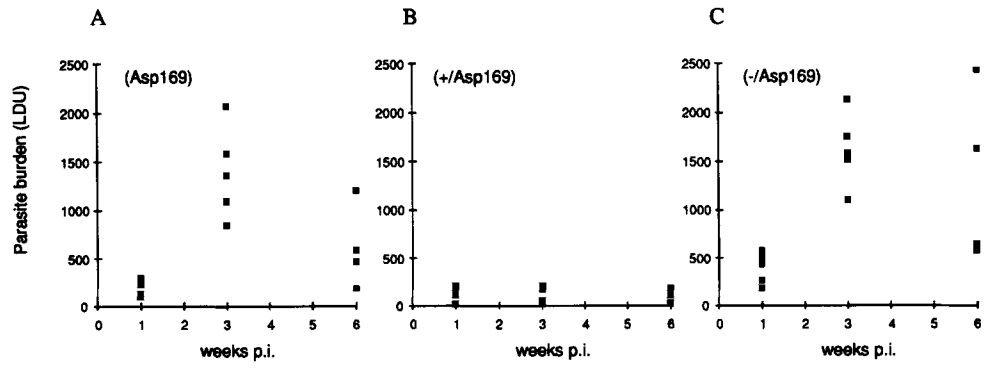

Figure 5. *L. donovani* infection in livers of control mice and mice bearing targeted mutations at *Nramp1*. Groups of either control susceptible BALB/cJ mice (Asp169, *A*) or resistant (129sv × BALB/cJ) F1 (+/Asp169, *B*) mice, and mice from a (129sv × BALB/cJ) F2 cross heterozygous (−/Asp169, *C*) for a null allele at *Nramp1*, were tested for resistance to infection with *L. donovani*. 1 × 10^7 live *L. donovani* amastigotes were injected intravenously, and the parasitemia was followed in the liver by determining the number of LDU (number of amastigotes/1,000 scored cell nuclei) in fresh imprints of this organ at different times after infection (*p.i.*). The results from individual animals of groups of three to five mice are shown.

gotes (129sv × BALB/c) F1 mutants (*Nramp1*$^{-/Asp169}$), the profile of *L. donovani* infection was very similar to that observed in BALB/c controls (Fig. 5 *A*), including rapid parasite proliferation in the early phase peaking at 3 wk, followed by a reduction in the liver parasite load by 6 wk after infection. These results clearly indicate that disruption of *Nramp1* abrogates natural resistance to *L. donovani* infection, demonstrating that *Lsh* and *Nramp1* are the same gene.

As opposed to infections with mycobacteria or *L. donovani*, *S. typhimurium* is a highly virulent mouse pathogen that replicates very rapidly in RE organs and produces an overwhelming and rapidly lethal infection in susceptible mouse strains (8). Other inbred mouse strains are completely resistant and survive an infectious challenge well. In this infection, the differential growth of the microbe in the early phase of the infection is critical for survival of the animals, since the infection is rapid and does not allow for the establishment of specific immune response as with the other two infectious models analyzed. The dramatic difference in bacterial growth rates is genetically controlled by the *Ity* gene, which maps very closely to or is identical to *Lsh* and *Bcg*.

Since the *Ity* phenotype of the 129sv strain used in the targeting experiment was unknown, and since additional genetic loci can also modulate early replication of *S. typhimurium* in RE organs (see Discussion), we compared the degree of resistance/susceptibility to this infection of control C57Bl/6J and BALB/cJ mice (both *Ity*^{s}, *Nramp1*^{Asp169}) with that of (129sv × BALB/c) F1 hybrids (*Ity*$^{s/s}$, *Nramp1*$^{+/Asp169}$). Results in Fig. 6 (experiment *A*) show that control C57BL/6J and BALB/c mice quickly succumbed to this infectious inoculum, with no animal from these two groups surviving more than 6 d. In contrast, all (129sv × BALB/c) F1 animals survived this period and were still healthy 2 wk after infection (end of observation period). This indicated that 129sv mice carry the *Ity*^{r} allele, in agreement with previous haplotype-typing data (20). Results from experiment *B* in Fig. 6 indicated that disruption of the wild-type 129sv *Nramp1* allele in (129sv × BALB/c) F1 mice (*Nramp1*$^{-/Asp169}$) abrogated their resistance to *S. typhimurium* infection, and all animals of this group quickly succumbed to infection within a time span identical to that observed in susceptible BALB/c controls. Finally, analysis of resistance to infection in homozygous *Nramp1*$^{-/-}$ mutants in a third experiment (Fig. 6 *C*) also indicated acute sensitivity to *S. typhimurium* infection. These results establish that *Nramp1* and *Ity* are allelic.

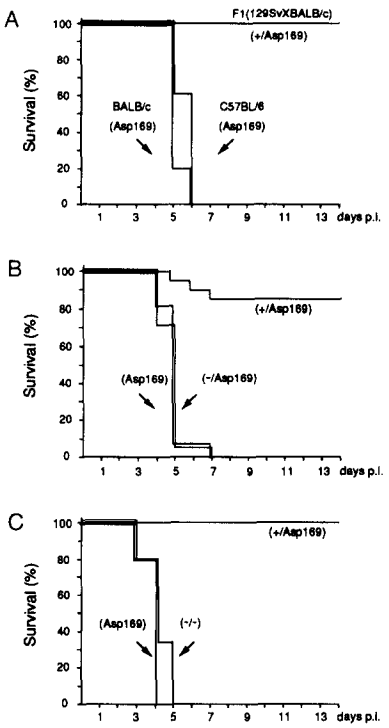

Figure 6. *S. typhimurium* infection in control mice and mice bearing targeted mutations at *Nramp1*. Groups of either control susceptible BALB/cJ and C57BL/6J or control resistant (129sv × BALB/cJ) F1 mice, or mice from a (129sv × BALB/cJ) F2 cross either heterozygous (−/Asp169) or homozygous (−/−) for a null allele at *Nramp1*, were tested for resistance to infection with *S. typhimurium* in three separate experiments (numbered *A*–*C*). 1 × 10^{4} live *S. typhimurium* bacilli (CFU) were injected intravenously into groups of 5–15 mice, and animals either moribund or succumbing to infection were recorded twice a day. The data are expressed as the proportion of animals surviving the infection and are shown as the percentage of survival.

Discussion

Nramp1 and Bcg Are Allelic. *Nramp1* was identified as a likely candidate for *Bcg* (17) as a result of the following observations: (*a*) It mapped within the minimal genetic and physical intervals delineating the *Bcg* region; (*b*) it was expressed primarily in RE organs and macrophages; (*c*) a non-conservative glycine to aspartic acid substitution (G169D) within TM4 of the protein cosegregated with the *Bcg*^{r}/*Bcg*^{s} phenotype in 27 inbred strains analyzed (20); and (*d*) the G169D substitution fell within a region and at a residue highly conserved across *Nramp* homologues of other species (17, 20). Despite this evidence, the association between *Nramp1* and *Bcg* remained correlative, and logical counterarguments could be put forward: (*a*) The minimal physical interval for *Bcg* was estimated at 1.1 Mb, and only a 400-kb portion of it was cloned and searched for the presence of candidate genes. (*b*) The minimal physical interval for *Bcg* was later found to include other genes, the known functions of which made them very likely candidates for a disease resistance locus. For example, the gene family encoding the cell surface receptors for the key inflammatory lymphokine IL-8 was recently mapped to human 2q35 (*IL8RA*, *IL8RB*, *IL8RBP*; 34, 35) and to proximal mouse 1 (36, 37), within the *NRAMP-1/VIL1* interval (35). (*c*) The G169D substitution associated with the *Bcg*^{s} phenotype did not constitute an obvious loss of function, and a complete polypeptide was expected to be produced in *Bcg*^{s} mice. To formally test the candidacy of *Nramp1* as *Bcg*, we constructed a mouse mutant bearing a null allele at *Nramp1* and analyzed the effect of this mutation on the natural resistance to infection with *M. bovis* (BCG). These experiments demonstrate that *Nramp1* and *Bcg* are in-

deed allelic, therefore validating our overall experimental strategy for positional cloning of *Bcg*. As opposed to spontaneously arising or x ray–induced mutants with an obligatory phenotype and having only one or a few alleles, the genetic difference at *Bcg* is distributed among "normal" inbred strains and is only revealed upon environmental challenge through exposure to an infectious agent. As opposed to the former situation, in which a chromosomal landmark (deletion, inversion, translocation) or obvious non-sense mutation can guide the identification of the mutant gene, the latter situation may involve a more subtle change that can only be identified in haplotype-mapping studies, extensive nucleotide sequencing of the gene from many inbred strains, and final testing of candidate genes in gene-targeting experiments. This strategy (identification and study of segregation of allelic variants) is likely to prove useful for the identification of genetic differences among inbred strains that cause subtle phenotypes (behavioral traits), or for the study of more complex and polygenic traits, such as susceptibility to hypertension, diabetes, or neoplasia, where single mutations with obligatory phenotypes are rarely available.

Nramp1, Bcg, Ity, and Lsh Are Allelic. Although genetic factors have been implicated in resistance to benign and acute forms of leishmaniasis (7, 38, 39), the clearest manifestation of genetic control is for visceral leishmaniasis caused by *L. donovani*. While some mouse strains allow rapid proliferation of the parasites in liver, others completely inhibit parasite growth. This difference is controlled by the chromosome 1 locus *Lsh* (7), and in vitro experiments have shown that *Lsh* is expressed by the mature tissue macrophage (11). In the case of murine typhoid caused by *S. typhimurium*, three loci play a key role in susceptibility to infection and response to the bacterial LPS. Inbred strains either rapidly die of an overwhelming infection or completely survive challenge with a small intravenous inoculum of *S. typhimurium*. This difference is caused by a differential growth rate of the bacilli in RE organs and is controlled by the expression in macrophages of the *Ity* locus on chromosome 1 (8, 10, 40). Two additional genes have been shown to further modulate *S. typhimurium* resistance of Ity^r strains. The chromosome 4 locus *Lps*, which controls the LPS-induced cytotoxicity and production of immunomodulators such as IL-1, CSF, PGE-2 and TNF-α typical of activated macrophages, is deficient (Lps^d) in C3H/HeJ (for review see reference 41). In addition, a mutation in the *Btk* kinase gene (42, 43) of CBA/N mice (*xid*; 44) causes a failure to mount B cell–mediated antibody response against LPS, leading to a progressive and ultimately lethal infection. The phenotypic analysis of the *Lps* and *xid* mutations clearly indicates that, in addition to the genetic advantage conferred by Ity^r, both efficient LPS-induced macrophage activation and humoral response are essential for controlling and ultimately surviving *S. typhimurium* infection.

Genetic linkage studies have independently positioned *Ity*, *Lsh*, and *Bcg* to the same portion of proximal mouse 1 (33). Cosegregation analyses in 38 recombinant inbred strains or by successive infections in the same backcross mice (26 tested for *Bcg* and *Lsh*) or by progeny testing (25 families tested for *Bcg* and *Ity*) have failed to detect recombination between the three loci (33). However, the limited resolution of these analyses (200 meioses analyzed, maximum distance of 1 cM) has not allowed the distinguishing between allelism and tight linkage. Despite the similarities in phenotypic expression of the three loci in RE organs and macrophages, the lack of phylogenic links and the different physiopathology caused by the three infectious agents have made it difficult to envision a pleiotropic mechanism of action. Results from *L. donovani* and *S. typhimurium* infections in *Nramp1* null mutants (Figs. 5 and 6) demonstrate that *Nramp1*, *Bcg*, *Ity*, and *Lsh* are indeed the same gene. Therefore, *Nramp1* must fulfill a biochemical function that is key to the capacity of the macrophage either to restrict the growth or to actively kill these three unrelated microbes. A comparison of the intracellular fate of these three infectious agents may provide some clues as to a possible common site of action of *Nramp1*. Within a few min after phagocytosis, microbes are found included within a vacuole called the phagosome. This is followed by acidification of the phagosome to pH 5.5–5 and fusion to secondary lysosomes, resulting in further acidification (pH 4.5) and delivery of digestive enzymes to the vacuole. *Salmonella*, *Mycobacterium*, and *Leishmania* are all initially present in phagosomes but have devised mechanisms to escape the subsequent cytocidal pathway. *Mycobacterium* inhibits phagosome/lysosome (P/L) fusion (45–47) and completely inhibits phagosome acidification by either actively destroying the host vacuolar H+/ATPase or by selectively preventing fusion to H+/ATPase positive vesicles (47, 48). The intracellular fate of *Salmonella* is more controversial (49–51), but a strong correlation has been established between intracellular survival and inhibition of P/L fusion (50, 52). *Salmonella* is also capable of preventing phagosome acidification, although to a lesser extent than *Mycobacterium* (53). By contrast, *Leishmania* amastigotes inhibit neither P/L fusion nor phagosome acidification but can survive and multiply within fused P/L (54, 55), possibly through secretion of inhibitory molecules such as oxygen radical scavengers (for review see reference 56). Considering these different survival strategies, it is difficult to envision that a late step such as phagosome acidification and/or P/L fusion would be a likely site of *Nramp1* action. Therefore, an earlier step of the parasite–macrophage interaction such as the unfused phagosome stage may be a more likely site for *Nramp1* action, either through a cytostatic or cytocidal mechanism.

Nramp1 Function in the Early and Late Phases of Infection. Results in Figs. 4–6 clearly establish that *Nramp1* plays a major role in the early phase of infection, which, in the case of *S. typhimurium* infection, is absolutely critical, since animals rapidly die of overwhelming infection in its absence. However, the fact that neither BCG nor *L. donovani* infections are lethal for mice allows investigation of the effect of *Nramp1* disruption on the late "curative" or immune phase of infection (Figs. 4 and 5). During this period, infected macrophages produce IL-1β and TNF-α locally to induce granuloma formation and may act as APC to activate $CD4^+$ and/or $CD8^+$ T cells. Activated T cells produce a large

number of cytokines, most importantly IFN-γ and IL-2, which mediate the activation of macrophage bactericidal functions such as respiratory burst, nitric oxide synthesis, and production of a large number of proteases and other lysosomal enzymes. The key role of IFN-γ–mediated macrophage activation in eradication of these infections has been established in vivo and in vitro (57–60, 28). Our results indicate that *Nramp1* ablation impairs neither granuloma formation (Fig. 3) nor successful microbicidal response in this part of the infection (Figs. 4 and 5). Since activated macrophages are the key effector cells of this response, these results suggest that *Nramp1* does not play a major role in the elimination of intracellular parasites by activated macrophages. What biochemical mechanism of *Nramp1* action can be proposed to account for a key role during the early but not the late phase of infection can only be speculated upon. A possible cytocidal function mediated by *Nramp1* could play a major role early in infection, but may be redundant and may only form part of a number of additional cytocidal mechanisms expressed in the late phase after macrophage activation. The observation that *Nramp1* is constitutively expressed in macrophages but is dramatically induced by IFN-γ and LPS treatments is in agreement with a function for *Nramp1* in both resting and activated macrophages (Gros, P., and G. Govoni, unpublished observations). Alternatively, *Nramp1* could have a cytostatic rather than cytocidal function discernible only early during infection, and perhaps creating an intraphagosomal environment unfavorable to parasite replication. In support of a cytostatic function for *Nramp1* are metabolic labeling studies of *Leishmania* amastigotes in infected livers, where differences in rates of replication rather than of active elimination were associated with the genetic advantage of *Lsh*^{r} macrophages (61). Irrespective of the model, the study of *Nramp1* mutant mice clearly suggests a novel mechanism by which macrophages can control replication of taxonomically diverse microorganisms independently of the immune system.

Nramp1^{Asp169} *Is a Null Allele.* The observation that *Nramp1*^{Asp169} homozygotes, *Nramp1*$^{-/Asp169}$ heterozygotes, or *Nramp1*$^{-/-}$ homozygotes are equally susceptible to BCG, *Salmonella*, and *L. donovani* infections (Figs. 4–6) indicates that the G169D substitution is not a partial loss of function but is rather a null mutation at *Nramp1*. Nramp1 is a novel integral membrane protein, the salient predicted features of which include 12 TM domains, with 7 of them containing at least one charge, an extracellular glycosylated loop, and an intracellular consensus transport motif previously described in a large number of prokaryotic and eukaryotic membrane transporters. This suggests that Nramp1 performs a transport function in macrophages. We have recently determined that (*a*) *Nramp1* is a member of a family of three genes in rodents (19, 62) that encode highly conserved polypeptides (85% homology) (19); and (*b*) the *Nramp* family is extremely well conserved through evolution, with members identified in all animal species tested (75–90% homology), but also in distant eukaryotes such as plants, flies, and yeast (50–70% homology) (Gros, P., unpublished results). The predicted TM domains are the most conserved domains (up to 90% for homologues and 75% for orthologues), including the charged amino acids within them, which together suggest a key structural and/or functional role for these segments and residues in a common mechanism of action of these proteins (e.g., stabilization of unstable charges in the lipid bilayer; 63). The G169D substitution would replace a small neutral amino acid by a large residue with a charged side chain within predicted TM4 of Nramp1. Considering the high degree of evolutionary conservation of both the sequence and charges within TM domains, the introduction of an additional charged residue within a TM domain would be expected to have severe deleterious effects on protein function. This mutation could affect either proper targeting, insertion, or folding of Nramp1 within the membrane or may interfere with the intimate mechanism of transport of Nramp1.

Haplotype-mapping studies of genealogically and phylogenetically distant inbred mouse strains have indicated that *Bcg*^{s} strains share a common chromosome 1 haplotype around *Nramp1*. This suggests that the *Nramp1*^{Asp169} allele may have been present in several founders of the different inbred strains and had become randomly fixed in some strains. The persistence of the potentially deleterious Asp169 allele in inbred mouse strains or even in wild mice can be explained in two ways. First, although it is clear that the uncontrolled replication of intracellular parasites in RE organs typical of the Asp169 allele may have a dramatic deleterious effect on survival of *Salmonella* infection, it may be counterbalanced by positive secondary effects for other types of infection. Indeed, Asp169 animals may be more prone to mounting a vigorous immune response against certain benign infections, which in turn may advantageously cross-protect them against more virulent related organisms that may prove lethal to Gly169-bearing mice. Alternatively, it is possible that maintaining heterozygosity for one of the markers tightly linked to *Nramp1* and preserved in the haplotype-defining *Bcg*^{s} strains may confer a yet to be identified advantage over strains homozygous for the Gly169 allele. This advantage may have helped preserve the Asp169 in the breeding of inbred strains and may even have enabled its survival in the wild.

We wish to thank Dr. J. Rossant (Mount Sinai Hospital, Toronto, Canada) for the generous gift of the 129sv/J genomic I phage library, Dr. E. Li and Dr. R. Jaenisch (Whitehead Institute for Biomedical Research, Cambridge, MA) for the J1 ES cell line, Dr. G. Matlashewski (Institute of Parasitology, McGill University) for providing Syrian hamsters infected with *L. donovani*, and Dr. H. Robson (Royal Victoria Hospital, McGill University) for the gift of an *S. typhimurium* isolate. We would like to acknowledge M. Boulé, Eva Michaliszyn, and P. Brinkley for technical assistance.

This work was supported by research grants to P. Gros, E. Skamene, and M. L. Tremblay from the National Institutes of Health (5R01 AI35237.02). P. Gros is supported by an E. W. R. Steacie fellowship from the National Sciences and Engineering Research Council of Canada and is an International Research Scholar of the Howard Hughes Medical Institute. S. Vidal is supported by a fellowship from Canadian Genetic Diseases Network–Merck Frosst. M. L. Tremblay and D. Malo are recipients of career awards from the Fonds de la Recherche en Santé du Québec.

Address correspondence to Dr. P. Gros, Department of Biochemistry, McGill University, 3655 Drummond, Room 907, Montreal, Quebec, Canada H3G 1Y6.

Received for publication 3 April 1995.

References

1. Malo, D., and E. Skamene. 1994. Genetic control of host resistance to infection. *Trends Genet.* 10:365–371.
2. Gros, P., E. Skamene, and A. Forget. 1981. Genetic control of natural resistance to *Mycobacterium bovis* BCG. *J. Immunol.* 12:2417–2421.
3. Skamene, E., P. Gros, A. Forget, P.J. Patel, and M. Nesbitt. 1984. Regulation of resistance to leprosy by chromosome 1 locus in the mouse. *Immunogenetics.* 19:117–120.
4. Goto, Y., E. Buschman, and E. Skamene. 1989. Regulation of host resistance to *Mycobacterium intracellulare in vivo* and *in vitro* by the *Bcg* gene. *Immunogenetics.* 30:218–221.
5. Pelletier, M., A. Forget, D. Bourassa, P. Gros, and E. Skamene. 1982. Immunohistopathology study of *Mycobacterium bovis* (BCG) infection in innately resistant and susceptible mice. *J. Immunol.* 129:2179–2182.
6. Brett, S., J.M. Orrell, J. Swanson Beck, and J. Ivanyi. 1992. Influence of H-2 genes on growth of *Mycobacterium tuberculosis* in the lungs of chronically infected mice. *Immunology.* 76: 129–132.
7. Bradley, D.J. 1977. Genetic control of *Leishmania* populations within the host. II. Genetic control of acute susceptibility of mice to *L. donovani* infection. *Clin. Exp. Immunol.* 30:130–140.
8. Plant, J.E., and A. Glynn. 1976. Genetics of resistance to infection with *Salmonella typhimurium* in mice. *J. Infect. Dis.* 133:72–78.
9. Stach, J.L., P. Gros, A. Forget, and E. Skamene. 1984. Phenotypic expression of genetically controlled natural resistance to *Mycobacterium bovis* (BCG). *J. Immunol.* 132:888–892.
10. Lissner, C.R., R.N. Swanson, and A.D. O'Brien. 1983. Genetic control of the innate resistance of mice to *Salmonella typhimurium*: expression of the *Ity* gene in peritoneal and splenic macrophages isolated *in vitro*. *J. Immunol.* 131:3006–3013.
11. Olivier, M., and C.E. Tanner. 1987. Susceptibilities of macrophage populations to infection in vitro by *Leishmania donovani*. *Infect. Immun.* 55:467–471.
12. Gros, P., E. Skamene, and A. Forget. 1983. Cellular mechanisms of genetically-controlled host resistance to *Mycobacterium bovis* (BCG). *J. Immunol.* 131:1966–1973.
13. O'Brien, A.D., and E.S. Metcalf. 1982. Control of early Salmonella typhimurium growth in innately *Salmonella*-resistant mice does not require functional T lymphocytes. *J. Immunol.* 129:1349–1351.
14. Crocker, P.R., J.M. Blackwell, and D.J. Bradley. 1984. Transfer of innate resistance and susceptibility to *Leishmania donovani* infection in mouse radiation bone marrow chimaeras. *Immunology.* 52:417–422.
15. Malo, D., S.M. Vidal, J. Hu, E. Skamene, and P. Gros. 1993. High resolution linkage map in the vicinity of the host resistance locus *Bcg*. *Genomics.* 16:655–663.
16. Malo, D., S. Vidal, J.H. Lieman, D.C. Ward, and P. Gros. 1993. Physical delineation of the minimal chromosomal segment encompassing the murine host resistance locus *Bcg*. *Genomics.* 17:667–675.
17. Vidal, S.M., D. Malo, K. Vogan, E. Skamene, and P. Gros. 1993. Natural resistance to infection with intracellular parasites: identification of a candidate gene for *Bcg*. *Cell.* 73:469–485.
18. Unkles, S.E., K.L. Hawker, C. Grieve, E.I. Campbell, P. Montague, and J.R. Kinghorn. 1991. *crnA* encodes a nitrate transporter in *Aspergillus nidulans*. *Proc. Natl. Acad. Sci. USA.* 88:204–208.
19. Gruenheid, S., M. Cellier, S. Vidal, and P. Gros. 1995. Identification and characterization of a second mouse *Nramp* gene. *Genomics.* 25:514–525.
20. Malo, D., K. Vogan, S. Vidal, J. Hu, M. Cellier, E. Schurr, A. Fuks, N. Bumstead, K. Morgan, and P. Gros. 1994. Haplotype mapping and sequence analysis of the mouse *Nramp* gene predicts susceptibility to infection with intracellular parasites. *Genomics.* 23:51–61.
21. Li, E., T.H. Bestor, and R. Jaenisch. 1992. Targeted mutation of the DNA methyltransferase gene results in embryonic lethality. *Cell.* 69:915–926.
22. Love, P.E., M.L. Tremblay, and R. Westphal. 1992. Targeting of the T-cell receptor z-chain in embryonic stem cells: strategies for generating multiple mutations in a single gene. *Proc. Natl. Acad. Sci. USA.* 89:9929–9933.
23. Ramirez-Solis, R., J. Perez-Rivera, J.D. Wallace, M. Wims, H. Zheng, and A. Bradley. 1992. Genomic DNA microextraction: a method to screen numerous samples. *Anal. Biochem.* 201:331–335.
24. Sambrook, J., E.F. Fritsch, and T. Maniatis. 1989. Molecular Cloning: A Laboratory Manual. 2nd ed. C. Nolan, editor. Cold Spring Harbor Laboratory, Cold Spring Harbor, NY.
25. Feinberg, A.P., and B. Vogelstein. 1984. A technique for radiolabeling DNA restriction endonucleases fragments to high specific activity. *Anal. Biochem.* 132:6–13.
26. Tybulewicz, V.L.J., M.L. Tremblay, M.E. LaMarca, R. Willemsen, B.K. Stubblefields, S. Winfield, B. Zabloka, E. Sidransky, B.M. Martin, S.P. Huang, K.A. Mintzer, H. Westphal, R.C. Mulligan, and E.I. Ginns. 1992. Animal model of Gaucher's disease from targeted disruption of the mouse glucocerebrosidase gene. *Nature (Lond.).* 357:407–410.
27. Chirgwin, J.M., A.A. Przybyla, R.J. MacDonald, and W.J.

Rutter. 1979. Isolation of biologically active ribonucleic acid from sources enriched in ribonuclease. *Biochemistry.* 18:5294–5306.

28. Murray, H.W., J.J. Stern, K. Welte, B.Y. Rubin, S. Carriero, and C.F. Nathan. 1987. Experimental visceral leishmaniasis: production of interleukin 2 and interferon-gamma, tissue immune reaction, and response to treatment with interleukin 2 and interferon-gamma. *J. Immunol.* 138:2290–2297.
29. Robson, H.G., and S.I. Vas. 1972. Resistance of inbred mice strains to *Salmonella typhimurium*. *J. Infect. Dis.* 126:378–386.
30. Thomas, K.R., and M.R. Capecchi. 1987. Site-directed mutagenesis by gene targeting in mouse embryo-derived stem cells. *Cell.* 51:503–512.
31. Rook, G.A.W. 1990. The role of activated macrophages in protection and immunopathology in tuberculosis. *Res. Microbiol.* 141:253–256.
32. Wallis, R.S., and J.J. Ellner. 1994. Cytokines and tuberculosis. *J. Leukocyte Biol.* 55:676–681.
33. Skamene, E., P. Gros, A. Forget, P.A.L. Kongshavn, C. St.-Charles, and B.A. Taylor. 1982. Genetic regulation of resistance to intracellular pathogenes. *Nature (Lond.).* 297:506–509.
34. Morris, S.W., N. Nelson, M.B. Valentine, N.D. Shapiro, A.T. Look, C.J. Kozlosky, P.M. Beckmann, and D.P. Cerretti. 1992. Assignment of the genes encoding human interleukin-8 receptor types 1 and 2 and an interleukin-8 receptor pseudogene to chromosome 2q35. *Genomics.* 14:685–691.
35. White, J.K., M.-A. Shaw, C.H. Barton, D.P. Cerretti, H. Williams, B.A. Mock, N.P. Carter, C.S. Peacock, and J.M. Blackwell. 1994. Genetic and physical mapping of 2q35 in the region of the *NRAMP* and *IL8R* genes: identification of a polymorphic repeat in exon 2 of *NRAMP*. *Genomics.* 24:295–302.
36. Wilkie, T.M., Y. Chen, D.J. Gilbert, K.J. Moore, L. Yu, M.I. Simon, N.G. Copeland, and N.A. Jenkins. 1993. Identification, chromosomal location, and genome organization of mammalian G-protein-coupled receptors. *Genomics.* 18:175–184.
37. Cerretti, D.P., N. Nelson, C.J. Kozlosky, P.J. Morrissey, N.G. Copeland, D.J. Gilbert, N.A. Jenkins, J.K. Dosik, and B.A. Mock. 1993. The murine homologue of the human interleukin-8 receptor type B maps near the *Ity-Lsh-Bcg* disease resistance locus. *Genomics.* 18:410–413.
38. Blackwell, J.M., J. Freeman, and D. Bradley. 1980. Influence of H-2 complex on acquired resistance to *Leishmania donovani* infection in mice. *Nature (Lond.).* 283:72–74.
39. Roberts, M., B.A. Mock, and M.J. Blackwell. 1993. Mapping of genes controlling *Leishmania major* infection in CXS recombinant mice. *Eur. J. Immunogenet.* 20:349–362.
40. Plant, J., and A.A. Glynn. 1979. Locating *Salmonella* resistance gene on mouse chromosome 1. *Clin. Exp. Immunol.* 37:1–6.
41. Sultzer, B.M., R. Castagna, J. Bandekar, and P. Wong. 1993. Lipopolysaccharide nonresponder cells: the C3H/HeJ defect. *Immunobiology.* 187:257–271.
42. Thomas, J.D., P. Sideras, C.I.E. Smith, I. Vorechovsky, V. Chapman, and W.E. Paul. 1993. Colocalization of X-linked agammaglobulinemia and X-linked immunodeficiency genes. *Science (Wash. DC).* 261:355–358.
43. Rawlings, D.J., D.C. Saffran, S. Tsukada, D.A. Largaespada, and J.C. Grimaldi. 1993. Mutation of unique region of Bruton's tyrosine kinase in immunodeficient XID mice. *Science (Wash. DC).* 261:358–361.
44. O'Brien, A.D., I. Scher, and E.S. Metcalf. 1981. Genetically conferred defect in anti-*Salmonella* antibody formation renders CBA/N mice innately susceptible to *Salmonella typhimurium* infection. *J. Immunol.* 126:1368–1372.
45. Frehel, C., C. de Chastellier, T. Lang, and N. Rastogi. 1986. Evidence for inhibition of fusion of lysosomal and prelysosomal compartments with phagosomes in macrophages infected with pathogenic *Mycobacterium avium*. *Infect. Immun.* 52:252–262.
46. Sibley, L.D., S.G. Franzblau, and J.L. Krahenbuhl. 1987. Intracellular fate of *Mycobacterium leprae* in normal and activated mouse macrophages. *Infect. Immun.* 51:461–469.
47. Sturgill-Koszycki, S., P.H. Schlesinger, P. Chakraborty, L.H. Pryce, H.L. Collins, A.K. Fok, R.D. Allen, S.L. Gluck, J. Heuser, and D.G. Russell. 1994. Lack of acidification in *Mycobacterium* phagosomes produced by exclusion of the vesicular proton-ATPase. *Science (Wash. DC).* 263:678–681.
48. Xu, S., A. Cooper, S. Sturgill-Koszycki, T. van Heyninger, D. Chatterjee, I. Orme, P. Allen, and D.G. Russell. 1994. Intracellular trafficking in *Mycobacterium tuberculosis* and *Mycobacterium avium*-infected macrophages. *J. Immunol.* 153:2568–2578.
49. Carrol, M.E.W., P.S. Jackett, V.R. Aber, and D.B. Lowrie. 1979. Phagolysosome formation, cyclic adenosine 3′:5′-monophosphate and the fate of *Salmonella typhimurium* within mouse peritoneal macrophages. *J. Gen. Microbiol.* 110:421–429.
50. Buchmeier, N.A., and F. Heffron. 1991. Inhibition of macrophage phagosome-lysosome fusion by *Salmonella typhimurium*. *Infect. Immun.* 59:2232–2238.
51. Isberg, R.R., and G.T. Van Nhieu. 1994. Two mammalian cell internalization strategies used by pathogenic bacteria. *Annu. Rev. Genet.* 27:395–442.
52. Ishibashi, Y., and T. Arai. 1990. Specific inhibition of phagosome-lysosome fusion in murine macrophages mediated by *Salmonella typhimurium* infection. *FEMS (Fed. Eur. Microbiol. Soc.) Microbiol. Immunol.* 64:35–44.
53. Alpuche Aranda, C.M., J.A. Swanson, W.P. Loomis, and S.I. Miller. 1992. *Salmonella typhimurium* activates virulence gene transcription within acidified macrophage phagosomes. *Proc. Natl. Acad. Sci. USA.* 89:10079–10083.
54. Antoine, J.C., E. Prina, C. Jouanne, and P. Bongrand. 1990. Parasitophorous vacuoles of *Leishmania amazonensis*-infected macrophages maintain an acidic pH. *Infect. Immun.* 58:779–787.
55. Russell, D.G., S. Xu, and P. Chakraborty. 1992. Intracellular trafficking and the parasitophorous vacuole of *Leishmania mexicana*-infected macrophages. *J. Cell Sci.* 103:1193–1210.
56. Mauel, J. 1990. Macrophage-parasite interactions in *Leishmania* infections. *J. Leukocyte Biol.* 47:187–193.
57. Flesch, I.E.A., and S.H.E. Kaufman. 1990. Activation of tuberculostatic macrophage functions by gamma interferon, IL-4, and tumor necrosis factor. *Infect. Immun.* 58:2675–2677.
58. Cooper, A.M., D.K. Dalton, T.A. Stewart, J.P. Griffin, D.G. Russell, and I.M. Orme. 1993. Disseminated tuberculosis in interferon g gene-disrupted mice. *J. Exp. Med.* 178:2243–2247.
59. Flynn, J.-A.L., J. Chan, K.J. Triebold, D.K. Dalton, T.A. Stewart, and B.R. Bloom. 1993. An essential role for interferon g in resistance to *Mycobacterium tuberculosis* infection. *J. Exp. Med.* 178:2249–2254.
60. Murray, H.W., B.Y. Rubin, and C.D. Rothermel. 1983. Killing of intracellular *Leishmania donovani* by lymphokine-stimulated human mononuclear phagocytes. Evidence that interferon g is the activating lymphokine. *J. Clin. Invest.* 72:1506–1510.
61. Bradley, D.J.R. 1979. Regulation of *Leishmania* populations within the host. IV. Parasite and host cell kinetics studied by radioisotope labeling. *Acta Trop.* 36:171–179.
62. Dosik, J.K., C.H. Barton, D.L. Holiday, M.M. Krall, J.M. Blackwell, and B.A. Mock. 1994. An *Nramp*-related sequence maps to mouse chromosome 17. *Mamm. Genome.* 5:458–460.
63. Sahin-Toth, M., R.L. Dunten, A. Gonzalez, and H.R. Kaback. 1992. Functional interactions between putative intramembrane charged residues in the lactose permease of *Escherichia coli*. *Proc. Natl. Acad. Sci. USA.* 89:10547–10551.